common defect type, while in the non-polar a-GaN layers most of the defects are (0001)-oriented stacking faults [1].

We developed a method for the determination of the densities of individual defect types both in c- and a-oriented GaN layers, based on diffuse x-ray scattering and reciprocal space mapping. In the c-GaN layers the method is based on the comparison of the reciprocal space map of the diffusely scattered intensity measured both in standard and grazing-incidence geometry, with simulations based on a numerical Monte-Carlo procedure [2], [3]. The density and type of stacking faults in a-GaN layers can be determined from the intensity distribution along [0001]-oriented streaks in reciprocal space perpendicular to the fault planes.

We have measured a series of GaN layers of both orientations with various defect densities and compared the densities resulting from our procedure with results of other independent methods (transmission electron micrography, etching techniques) and we obtain comparable total densities of defects.

[1] M.A. Moram, M.E. Vickers, *Reports on Progress in Physics* **2009**, *72,* 036502. [2] M. Barchuk, V. Holý, B. Miljevic, B. Krause, T. Baumbach, J. Hertkorn, F. Scholz, *J. Appl. Phys.* **2010**, *108,* 043521. [3] M. Barchuk, V. Holý, B. Miljevic, B. Krause, T. Baumbach, *Appl. Phys. Lett.* **2011**, *98,* 021912.

Keywords: gallium nitride, diffuse X-ray scattering, defects

MS.28.3

Acta Cryst. (2011) A**67,** C74

Lithium niobate: a smart material for various applications in optoelectronics

Marc D Fontana, Sabrina Mignoni, Rachid Hammoum, Patrice Bourson, *Laboratoire Matériaux Optiques, Photonique et Systèmes, Université Paul Verlaine – Metz and Supélec, 2 rue Edouard Belin, 57070 Metz (France).* E-mail: fontana@metz.supelec.fr

$LiNbO_3$ (LN) is a widely studied optoelectronic material useful for a great variety of applications in non linear optics, integrated optics and solid state lasers [1], [2]. It can be grown in large single crystals, usually by Czochralski technique, and generally in the congruent composition [3]. Therefore it presents a Li deficiency and thus can be easily doped with various impurities. Doping these crystals can suitably change their optical properties [2]. Thus doping LN with rare earth ions or Cr is appropriate to induce luminescence. The introduction of Fe gives rise to a large photorefractive effect, whereas doping with Mg or Zn provides electrooptic coefficients with an efficient use [1], [2].

In fact the incorporation of dopants induces a change in the local structure of intrinsic (lattice) defects related to non-stoichiometry [4]. The congruent composition corresponds to a composition of nearly 0.94, meaning that about 6% of Li sites are empty. Since Nb^{5+} ions have a radius close to Li^+, they can go fill these empty sites (they are called antisites defects). Different models were proposed to describe the intrinsic defects in the nominally pure crystals with different compensation mechanisms: Li vacancy model or Nb vacancy model for the congruent composition [3] and coexisting Li and Nb vacancies with a content varying with the composition from congruent to stoichiometric [5]. The incorporation of dopants in the LN lattice does not have the same effect since it enters the A site (generally occupied by Li ions) or the B site (generally occupied by Nb ions) according to the nature and the concentration of the dopants. As a consequence, it induces different changes in the dynamics of intrinsic defects: Nb and Li vacancies, Nb antisites.

Here are pointed out the dependencies of several linear and non linear optical properties on the dopant content. The electrooptic and photorefractive [6-8] properties recorded in LN crystals doped with Mg, Fe, Zn or Hf [9], [10] are especially reported and discussed. The link between the mechanism and site of incorporation of dopants and the non-monotonous behaviour of optical properties is demonstrated. Thus the remove of antisite defects is related to a threshold in the behaviour of some optical properties.

At last is shown how the optimization of the structure can be used in applications in optoelectronics.

[1] E. Kratzig, O.F. Schirmer, *Photorefractive Materials and Their Applications, Topics in AppliedPhysics,* Springer-Verlag, Berlin, **1999**, *62*, 131-166. [2] T. Volk, M. Wöhlecke, *Lithium Niobate Defects, Photorefraction and Ferroelectric Switching,* Springer Berlin Heidelberg, **2008.** [3] A. Räuber, *Chemistry and physics of lithium niobate, Current Topics in Material Sciences,* Ed. by E. Kaldis, North Holland, Amsterdam, **1978**, 481-601. [4] Y. Zhang, L. Guilbert, P. Bourson, K. Polgar, M.D. Fontana, *J. Phys.: Condens. Matter* **2006**, *18*, 957-963. [5] F. Abdi, M.D. Fontana, M. Aillerie, P. Bourson, *Applied Physics A* **2006**, *83, 3*, 427-434. [6] M. Abarkan, M. Aillerie, J.-P. Salvestrini, M.D. Fontana, E. Kokanyan, *Applied Physics B: Lasers and Optics* **2008**, *92,* 603-608. [7] R. Mouras, M.D. Fontana, M. Mostefa, P. Bourson, *J. Opt. Soc. Am. B* **2006**, *23, 3*, 1867-1871. [8] F. Abdi, M. Aillerie, P. Bourson, M.D. Fontana, *Journal of Applied Physics,* **2009**, *106*, 033519. [9] R. Hammoum, M.D. Fontana, M. Gilliot, P. Bourson, E. Kokanyan, *Solid State Communications,* **2009**, *149,* 1967-1970. [10] S. Mignoni, M.D. Fontana, M. Bazzan, M.V. Ciampolillo, A.M. Zaltron, N. Argiolas, C. Sada, *Applied Physics B: Lasers and Optics,* **2010,** *101*, 541-546.

Keywords: defect, optoelectronics, doped

MS.28.4

Acta Cryst. (2011) A**67,** C74-C75

Study of the thermal anisotropy of $KLu(WO_4)_2$ for high power laser applications

M. Aguiló, M. C. Pujol, X. Mateos, J. J. Carvajal, F. Díaz, *Física i Cristal·lografia de Materials i Nanomaterials (FiCMA-FiCNA-EMAS), Universitat Rovira i Virgili (URV), Campus Sescelades, c/ Marcel.lí Domingo, s/n, E-43007 Tarragona, (Spain).* E-mail: Magdalena.aguilo@urv.cat

$KLu(WO_4)_2$ crystal belongs to the monoclinic system, with the space group *C*2/*c*. This material is a well known interesting laser host material for optically active lanthanides ions, such as Yb^{3+} and Tm^{3+}. Successful laser action of both ions, at 1.1 microns and 1.9 microns has been already demonstrated, in different configurations such as slab, waveguide and thin disk and also, in continuous-wave (cw) and pulsed regimes. Nevertheless, the complete knowledge of the physical anisotropy of this material and its application in laser action can lead to further improvements in laser efficiency or new applications. In relation with this aspect, the study of the thermal anisotropy of this material is crucial. Thermal conductivity in this crystal is a symmetrical second-rank tensor and as the crystal is monoclinic it has four nonzero components in the crystallo-physical frame $X_{1\kappa}$//***a***., $X_{2\kappa}$//***b***, $X_{3\kappa}$//***c****. With the measurement of the thermal diffusivity along four crystallographic directions (***a***, ***b***, ***c*** and ***c****), and the specific heat capacity, the thermal conductivity tensor has been calculated.

KLuW is grown from high temperature solutions. The solvent used by us is $K_2W_2O_7$ and the growth method was the Top Seeded Solution Growth by Slow Cooling (TSSG-SC). Samples for each measurement are crystallographically oriented to be cut and polished to optical grade quality. The eigenvalues of the thermal conductivity are κ'_{11}=2.95 $Wm^{-1}K^{-1}$, κ'_{22}=2.36 $Wm^{-1}K^{-1}$, and κ'_{33}=4.06 $Wm^{-1}K^{-1}$, with the maximum value along a direction in the ***a-c*** crystallographic plane, at 40.75° from the $\boldsymbol{N}_g$ principal optical axis (22.25º from c crystallographic axis), figure 1 shows the location of the tensor. KLuW is a optical biaxial crystal, in which the reference system for laser applications and linear optics is the real refractive index part, so the three principal optical directions,

which are N_g, N_m and N_p. N_p corresponds to the ***b*** crystallographic directions, and N_g and N_m are located in the (010) plane; N_g is located 18.5º clockwise from c crystallographic direction.

Such a thermal anisotropy in the monoclinic double tungstates leads to thermal lensing at high power operating levels. Focusing of the light in the crystal provokes high intensities so that the temperature increases significantly producing a mechanical deformation of the crystal, which in consequence, leads to a self-lensing material.

The laser experiments for power scaling carried out with Yb:KLuW in the thin disk configuration at high pump powers reached 9 W in cw regime showing a significant improvement in the thermal management due to the one-dimensional heat flow. This could be known thanks to the deep knowledge on the thermal properties of the monoclinic double tungstate crystals.

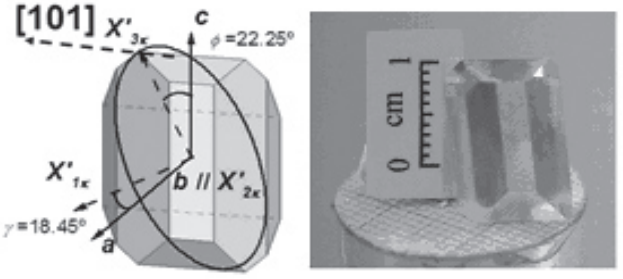

Keywords: thermal anisotropy, double tungstate crystals, high power lasers

MS.28.5

Acta Cryst. (2011) A**67,** C75

The optical spectra of $Sr_2SiO_4:Eu^{2+}$ nanocrystals

Young Jin Kim, Jun Seong Lee, *Department of Materials Science and Engineering, Kyonggi University, Suwon 443-760 (Korea).* E-mail: yjkim@kyonggi.ac.kr

Sr_2SiO_4 has two polymorphs: β-Sr_2SiO_4 (monoclinic) and α'-Sr_2SiO_4 (orthorhombic). There are two Sr^{2+} sites of ten-coordinated Sr(I) and nine-coordinated Sr(II) by oxygen atoms, which result in two emission bands at around 490 nm and 560 nm by doping Eu^{2+} ions. The various synthesizing methods such as a solid-state reaction and chemical preparations have been widely reported.

In this work, $Sr_2SiO_4:Eu^{2+}$ nanocrystals were prepared by a co-precipitation method using metal nitrates and 3-aminopropyltriethoxysilane (APTES) as a silicon source. NH_4Cl was used as a flux. The as-prepared powders were annealed with different temperatures under H_2 atmosphere in an electric tube furnace. The particle size and morphology were observed by a field-emission scanning electron microscope. X-ray diffractometer (XRD) and photoluminescence (PL) system were used to determine the crystal structure and the photoluminescence spectra, respectively. The effects of the preparation parameters on the structure of the nanocrystals and luminescent properties were investigated. With increasing the annealing temperature the crystallinity was enhanced, showing thin nanorod with the high aspect ratio. The PL spectra exhibited two emission bands at around 485 and 540 nm, indicating that Eu^{2+} ions were successfully substituted for two cation sites of Sr(I) and Sr(II). The preference of Eu^{2+} ions for Sr(I) or Sr(II) strongly depended on the preparing parameters such as the amount of a flux, firing temperature/time, and the Eu^{2+} concentration.

Keywords: luminescence, strontium, silicate

MS.29.1

Acta Cryst. (2011) A**67,** C75

Perspectives on the crystal structure of human adenovirus

Vijay S. Reddy, S. Kundhavai Natchiar, Tina-Marie Mullen, Glen R. Nemerow *The Scripps Research Institute, 10550 North Torrey Pines Road, La Jolla, California, 92037, (USA).*

Replication-defective and conditionally replicating adenovirus (AdV) vectors are currently being utilized in ~25% of human gene transfer clinical trials. Rational development of adenovirus vectors for therapeutic gene transfer is hampered by the lack of accurate structural information. The recently determined X-ray structure of an adenovirus vector at 3.5 Å resolution of the 150-MDa virion containing nearly 1 million amino acids represents a milestone as the biggest bio-molecular structure yet determined using X-ray diffraction methods (Reddy et al., 2010). The crystal structure revealed interactions between the major capsid protein (hexon) and characteristic structural elements of several accessory molecules that stabilize the AdV capsid. Interestingly, the virus structure also showed an altered association, a symmetry mismatch, between the 5-fold symmetric penton-base proteins and the 3-fold symmetric fiber proteins, where the trimeric shaft of the fiber proteins was seen buried deep inside pore formed by the penton base subunits at the particle vertices. The near atomic resolution structure highlights significant advances in understanding the stabilizing interactions, virus assembly and cell entry mechanisms of a large dsDNA virus and provides new opportunities for improving adenovirus-mediated gene transfer.

V.S. Reddy, S.K. Natchiar, P.L. Stewart, G.R. Nemerow *Science* **2010**, *329(5995),* 1071-5.

Keywords: adenovirus, capsid, structure

MS.29.2

Acta Cryst. (2011) A**67,** C75-C76

Structures of porcine adenovirus type 4 and bacteriophage T4 long tail fibres

Mark J. van Raaij,[a] Pablo Guardado-Calvo,[b] Sergio G. Bartual,[b] José M. Otero,[b] Carmela Garcia-Doval,[a] Antonio L. Llamas-Saiz,[c] Gavin C. Fox,[d] [a]*Departamento de Estructura de Macromoléculas, Centro Nacional de Biotecnología, CSIC, Madrid (Spain).* [b]*Departamento de Bioquímica y Biología Molecular, Universidad de Santiago de Compostela (Spain).* [c]*Unidad de Rayos X, RAIDT, Universidad de Santiago de Compostela (Spain).* [b]*Laboratoire de Proteines Membranaires, Institut de Biologie Structurale, Grenoble (France).* E-mail: mjvanraaij@cnb.csic.es

Certain viruses and bacteriophages use fibre proteins to bind to their host receptors. Examples are adenovirus, reovirus, and the T-even bacteriophages. These trimeric fibres have been shown to contain novel triple-stranded beta-structures. Here we present structures of porcine adenovirus type 4 fibre and of the tip of the bacteriophage T4 long tail fibre.

Adenovirus isolate NADC-1, a strain of porcine adenovirus type 4, has a fibre containing an N-terminal virus attachment region, shaft and head domains, and a C-terminal galectin domain connected to the head by an RGD-containing sequence. The crystal structure of the head domain is similar to previously solved adenovirus fibre head domains, but specific residues for binding the coxsackievirus and adenovirus receptor (CAR), CD46, or sialic acid are not conserved. The structure of the galectin domain reveals an interaction interface between its two